

PAPER • OPEN ACCESS

## Preparation and Photocatalytic Activity of BiOBr with High Exposure {102} Crystalline Surface

To cite this article: Chunhua Yuan *et al* 2019 *IOP Conf. Ser.: Mater. Sci. Eng.* **585** 012040

View the [article online](#) for updates and enhancements.

# Preparation and Photocatalytic Activity of BiOBr with High Exposure {102} Crystalline Surface

Chunhua Yuan, Hongling Bao, Yongqing Ren

College of Chemistry and Chemical Engineering, Inner Mongolia University of Science & Technology, Baotou, 014010, China  
Email: yuanchunhua79@126.com

**Abstract.** Flake BiOBr was prepared by one-step hydrothermal method using NaBr and  $\text{Bi}(\text{NO}_3)_3 \cdot 5\text{H}_2\text{O}$  as raw materials. The structure of the samples was characterized by means of XRD, SEM, UV-VIS. The photocatalytic activity of BiOBr was studied with methylene blue as probe. The results show that BiOBr with high exposure {102} can be obtained when the hydrothermal temperature of the product is 160 °C and the hydrothermal time is 24 h. Under visible light, the degradation rate of methylene blue was over 98%. When the catalyst was reused three times, the degradation rate could still reach 80%.

## 1. Introduction

BiOBr semiconductor materials have a tetragonal PbFCl structure [1]. A layer of  $[\text{Bi}_2\text{O}_2]$  is inserted between the two halogen atom layers, and then the  $[\text{X-Bi-O-Bi-Br}]$  sheets interact with each other by the van der Waals force between the Br atoms, layered semiconductor BiOBr is formed. In every single layer of  $[\text{Br-Bi-O-Bi-Br}]$ , there must be four oxygen atoms and four Br atoms around a bismuth atom to form asymmetric decahedral geometry [2]. The interaction between the  $[\text{Bi}_2\text{O}_2]$  layer and the layer is provided by covalent bonds, but the  $[\text{Br}]$  layer aggregation is provided by van der Waals force [3]. This structure can induce the generation of internal electric field, which is conducive to enhancing the separation efficiency of carriers. In addition, it belongs to indirect transition bandgap semiconductor [4]. Electrons must pass through some K layers to reach the valence band, which reduces the probability of photogenerated electron-hole recombination. In addition, because of the BiOBr bandgap width (2.8eV), visible light can be effectively utilized [5]. These characteristics enable BiOBr to effectively utilize sunlight, and it will have a good application prospect in visible light photocatalytic degradation of water pollutants.

In summary, because the morphology, size and crystallinity of BiOBr catalytic material affect its photocatalytic performance [6], BiOBr will be prepared by hydrothermal method. BiOBr with catalytic activity was prepared by controlling the preparation conditions, and then the photocatalytic degradation performance of BiOBr under visible light will be studied with methylene blue as a probe.

## 2. Materials and Methods

### 2.1 Materials

**Instruments:** electronic analytical balance (FA1004 Shanghai Hengping Scientific Instrument Co., Ltd), digital display thermostatic water bath (HH-6 Shanghai Pudong physical optics instrument factory), electric thermostatic drying oven (101 Beijing ever-bright medical instrument factory), X ray diffraction (Rigaku-12KW Japan), tungsten (40W Lianhua Lighting Co., Ltd.) 722s visible spectrophotometer (Shanghai precision scientific instrument Co., Ltd.). **Reagent:**  $\text{Bi}(\text{NO}_3)_3 \cdot 5\text{H}_2\text{O}$ ,



NaBr, Glacial acetic acid, absolute ethanol, methylene blue, methyl orange, rhodamine B, which was the analytical reagent.

### 2.2 Preparation of BiOBr Catalyst

Solution A is formed by dissolving 0.97 g  $\text{Bi}(\text{NO}_3)_3 \cdot 5\text{H}_2\text{O}$  in 3 mL glacial acetic acid. Solution B is formed by dissolving 0.24 g sodium bromide in 30 mL deionized water. The solution A is then rapidly poured into solution B to form a mixed solution. Mixed solution was fully stirred at room temperature for 30 minutes and then quickly moved into 100 ml stainless steel reactor with PTFE lining. The reactor was placed in the drying chamber for hydrothermal reaction, and the reaction temperature and time were controlled. After the reactor was cooled to room temperature, the product was washed and dried several times to obtain the finished product of BiOBr.

### 2.3 Characterization of Composite Materials BiOBr

The matter phase is analyzed by D/Max-3cX of X-ray powder diffraction (XRD), and SEM, and UV-visible absorption spectrum etc. The test conditions of XRD: Cu Target  $k_\alpha$  line, the Ni filter, the 40kV, 40mA, scanning range  $20^\circ \sim 80^\circ (2\theta)$ , scanning speed  $2^\circ/\text{min}$  using X-ray diffraction.

### 2.4 Photocatalytic Properties of Composite Materials BiOBr

40W tungsten lamp was used as a visible light source, and the light distance was 10 cm. The photocatalytic reaction process was: (1) a certain amount of BiOBr composite powder was added to the methylene blue solution of 10mg/L; (2) firstly, in the absence of light, the solution was ultrasonic dispersed for 3min and magnetic stirred for 10 min, so that the organic molecular reached adsorption/desorption equilibrium on the catalyst surface; (3) with the light source opening, the photocatalytic reaction was carried out at room temperature, and the suspension system was kept magnetic stirring during the whole process of the photocatalytic reaction; (4) every 20 min beginning the light open, 5 mL suspension sample was removed and centrifuged 10 min, then the upper liquid was absorbed, the solution absorbance of light catalytic was measured with 722S visible spectrophotometer in 665nm.

The degradation rate ( $\eta$ ) =  $(A_0 - A_1) / A_0 \times 100\%$

Type: The  $A_0$  and  $A_1$  was respectively absorbance value of before and after the degradation of methylene blue solution at the maximum absorption wavelength.

## 3. Results and Discussion

### 3.1 XRD Analysis of Composite Catalyst BiOBr

Figure 1 is the XRD analysis diagram of the product. Fig. 1 shows that all the BiOBr products are tetragonal, the highest peaks in a and b two-line diffraction peaks are {102} crystal planes, the diffraction peaks are sharp and there are no stray peaks. This shows that the product has good crystallinity and high purity. The product BiOBr is a flake structure growing along {102} plane orientation, and the larger the flake size of the product is, the higher the hydrothermal reaction temperature is. The photocatalytic experiment further proved that the more prominent {102} surface is, the better catalytic performance under visible light is. Analysis of curve B by jade 5.0, the half-height width of {102} diffraction peak is 0.134 and  $2\theta = 31.908$ . According to Scherrer's formula (where K is constant 0.89 and  $\lambda$  is 0.15405), the average diameter of BiOBr prepared at  $160^\circ\text{C}$  for 24 h is about 61 nm. BiOBr is a typical nanosheet structure.

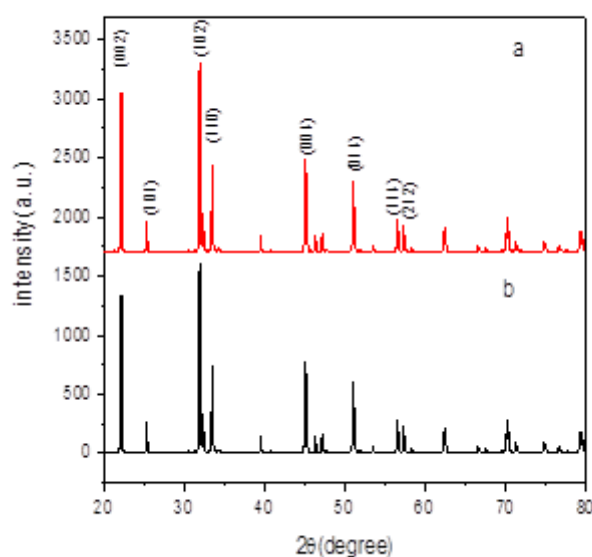


**Figure 1.** XRD of different preparation temperature BiOBr (a: 180 °C; b: 160 °C)

### 3.2 SEM Analysis of Composite Catalyst

Fig. 2 is the SEM diagram of BiOBr catalyst prepared at 180 °C, 160 °C and 140 °C, respectively, with hydrothermal reaction time of 24 h. Figure 2 shows that all the BiOBr produced in this experiment are in the shape of thin sheets, and the products are well dispersed without agglomeration. Further comparisons of figs. a, b and c in Fig. 2 show that the higher the hydrothermal reaction temperature is, the larger the crystal sheet is. When the temperature is 180 °C, the crystal particles are not uniform, and the size of the sample prepared at 160 °C is the most uniform. It was found that the catalytic performance of the product prepared at 160 °C was the best by testing its catalytic performance.

### 3.3 UV-Vis Diffuse Reflectance Spectra of Samples

Fig. 3 was the UV-visible absorption spectrum of different preparation temperature BiOBr composites, in which the preparation temperature was 180 °C, 160 °C. Figure 3 shows that the absorption range of BiOBr is about 320-440 nm, and the absorption range of products prepared at 160 °C is obviously red-shifted compared with those prepared at 180 °C. Figure 4 shows that the band gap of BiOBr prepared at 160 °C is 2.45 eV, that of BiOBr prepared at 180 °C is 2.65 eV, and that of standard BiOBr with tetragonal PbFCl structure is 2.8 eV. The results show that the band gap of BiOBr is effectively reduced and the visible photocatalytic efficiency is improved by controlling the growth of {102} crystal surface.

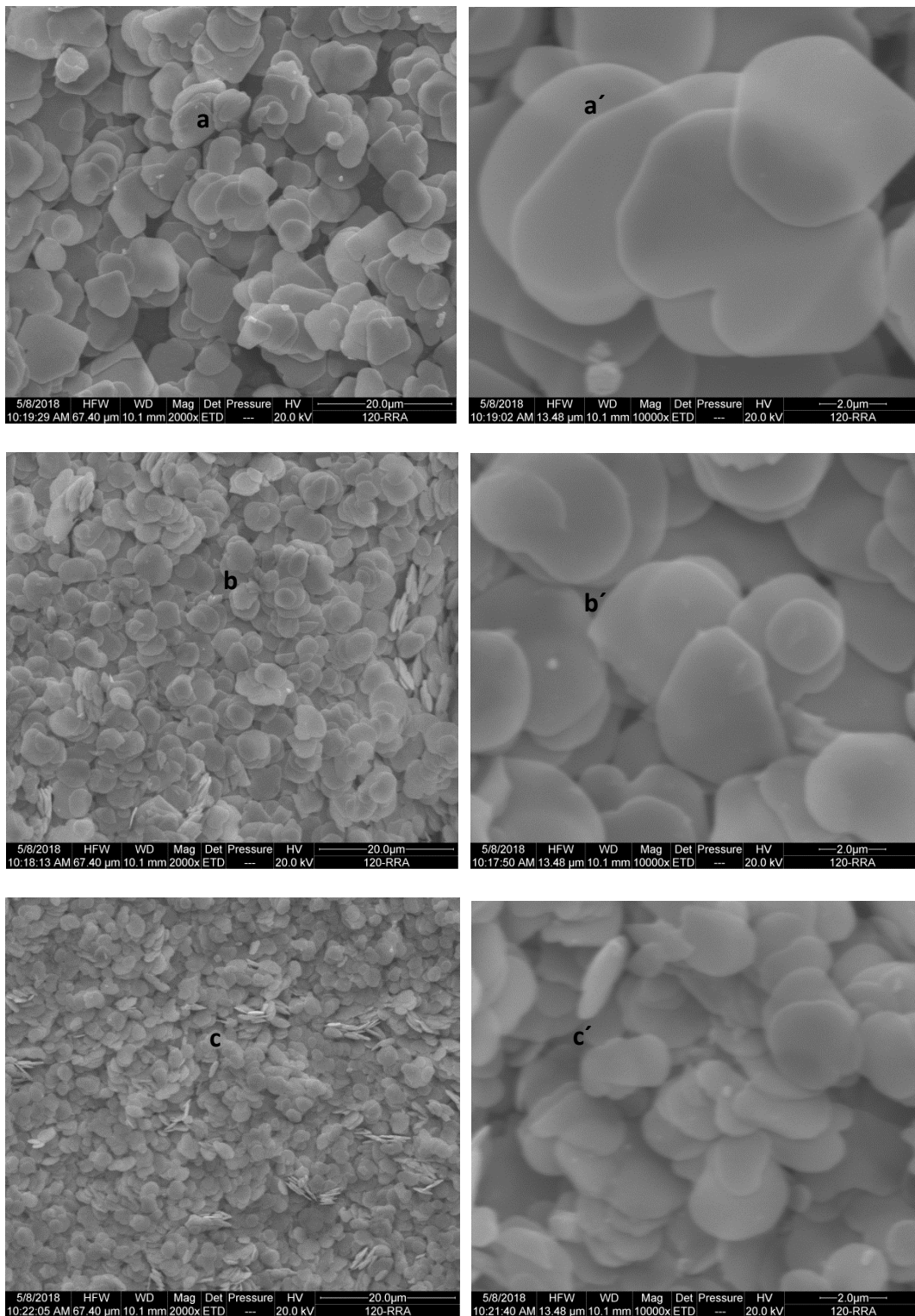


**Figure 2.** SEM images of different preparation temperature BiOBr (a, a 180 °C; b, b 160 °C; c, c 140 °C)

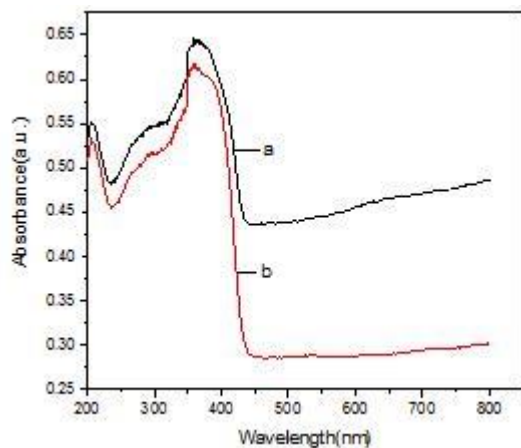


**Figure 3.** UV-Vis diffuse reflectance spectra Of different preparation temperature BiOBr (a: 160 °C b 180 °C)

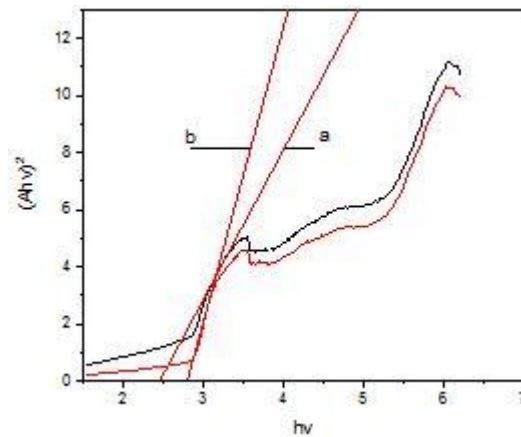
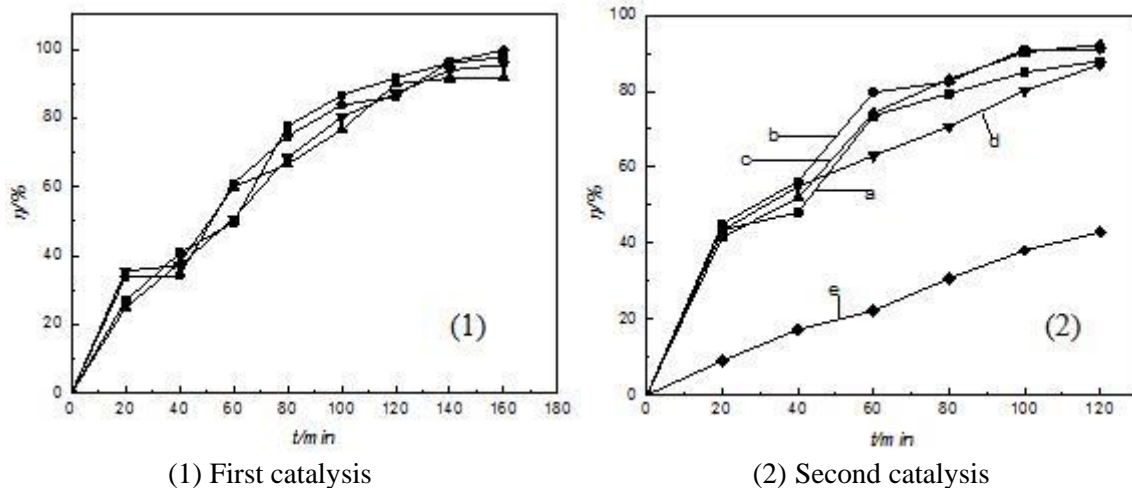


**Figure 4.**  $(Ahv)^2 - hv$  Of different preparation temperature BiOBr (a: 160 °C; b: 180 °C)

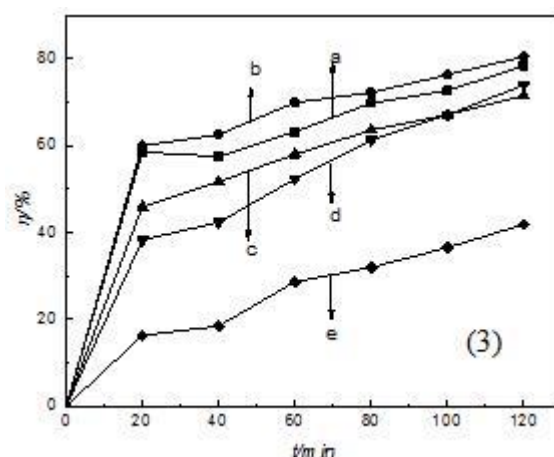
### 3.4 Study on Photocatalytic Properties of BiOBr

**3.4.1 Influence of Preparation Temperature on Photocatalytic Properties.** Fig.5 (1) primary photocatalytic degradation rate, (2) secondary recycling catalytic degradation rate, (3) tertiary recycling catalytic degradation rate. Fig.5 shows that the photocatalytic degradation rate of simulated dye wastewater can reach more than 98% when photocatalytic degradation is carried out with photocatalyst prepared at 160 °C and 24 h hydrothermal reaction time. After three times of recovery and reuse, the degradation rate of the catalyst for simulated dye wastewater can still reach 80%.



(1) First catalysis

(2) Second catalysis



(3) Third catalysis

**Figure 5.** Degradation rate of BiOBr at different preparation temperatures (a: 180 °C, b: 160 °C, c: 140 °C, d: 120 °C, e: blank)

**3.4.2 Influence of Preparation Time on Photocatalytic Properties.** Fig. 6 shows that the catalytic performance of the catalyst is better when the preparation time is controlled for 24 hours, because sufficient hydrothermal reaction time can make the crystal {102} surface grow more fully and the visible light photocatalytic efficiency is higher.

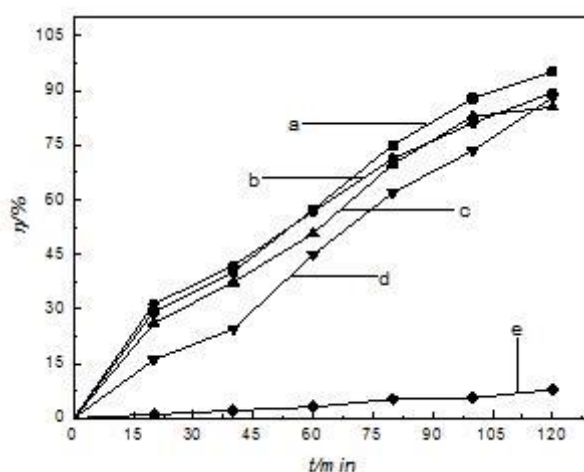


**Figure 6.** Degradation rate of BiOBr at different preparation time (a: 24 h, b: 16 h, c: 12 h, d: 8 h, e: Blank)

#### 4. Conclusions

(1) In this paper, NaBr and  $\text{Bi}(\text{NO}_3)_3 \cdot 5\text{H}_2\text{O}$  were used as raw materials to prepare high catalytic activity flake BiOBr by one-step hydrothermal method. High-speed growth {102} surface.

(2) The products were characterized by means of XRD, SEM and UV-VIS. The results show that Flake BiOBr with high-speed growth {102} surface can be obtained by controlling hydrothermal reaction time and temperature. The band gap of the product is 2.45eV, which can effectively reduce the band gap.

(3) The photocatalytic activity of BiOBr was studied using methylene blue as a probe. The catalytic performance of the product prepared under sunlight with hydrothermal temperature of 160 °C and hydrothermal time of 24 h was the best, and the degradation rate was over 98%. After three times of recovery and reuse, the degradation rate of the catalyst for simulated dye wastewater can still reach 80%.

## 5. Acknowledgment

This research was financially supported by the Natural Science Foundation of Inner Mongolia (No.2017MS(LH)0209).

## 6. References

- [1] An H. Z., Du Y. Photocatalytic properties of BiOX (X=Cl, Br and I). *Rare Metals*, 2008, 27 (3): 243-250.
- [2] Jing, Zhao K, Xiao X Y, et al. Synthesis and facet-dependent photoreactivity of BiOCl single-crystalline nanosheets [J]. *Journal of the American Chemical Society*, 2012, 134 (10): 4473-4476.
- [3] Li J, Zhang L Z, Li Y J, et al. Synthesis and internal electric field dependent photoreactivity of Bi<sub>3</sub>O<sub>4</sub> Cl single-crystalline nanosheets with high {001} facet exposure percentages [J]. *Nanoscale*, 2014, 6 (1): 167-171.
- [4] Kamat P V. TiO<sub>2</sub> nanostructures: recent physical chemistry advances [J]. *Journal of Physical Chemistry C*, 2012, 116 (22): 11849-11851.
- [5] Wang L, Li X, Wei T, et al. Efficient photocatalytic reduction of aqueous Cr(VI) over flower-like SnIn<sub>4</sub>S<sub>8</sub> microspheres under visible light illumination [J]. *Journal of Hazardous Materials*, 2013, 244-245 (2): 681-688.
- [6] Zhang J, Liu Y, Li Q, et al. Antifungal activity and mechanism of palladium-modified Nitrogen-doped Titanium oxide photocatalyst on agricultural pathogenic fungi fusarium graminearum [J]. *ACS Applied Materials & Interfaces*, 2013, 5 (21): 10953-10959.